



This is the accepted manuscript made available via CHORUS. The article has been published as:

## Space-Time Crystal and Space-Time Group

Shenglong Xu and Congjun Wu

Phys. Rev. Lett. **120**, 096401 — Published 27 February 2018

DOI: [10.1103/PhysRevLett.120.096401](https://doi.org/10.1103/PhysRevLett.120.096401)

# Space-time crystal and space-time group

Shenglong Xu and Congjun Wu

*Department of Physics, University of California, San Diego, California 92093, USA*

Crystal structures and the Bloch theorem play a fundamental role in condensed matter physics. We extend the static crystal to the dynamic “space-time” crystal characterized by the general intertwined space-time periodicities in  $D + 1$  dimensions, which include both the static crystal and the Floquet crystal as special cases. A new group structure dubbed “space-time” group is constructed to describe the discrete symmetries of space-time crystal. Compared to space and magnetic groups, space-time group is augmented by “time-screw” rotations and “time-glide” reflections involving fractional translations along the time direction. A complete classification of the 13 space-time groups in 1+1D is performed. The Kramers-type degeneracy can arise from the glide time-reversal symmetry without the half-integer spinor structure, which constrains the winding number patterns of spectral dispersions. In 2+1D, non-symmorphic space-time symmetries enforce spectral degeneracies, leading to protected Floquet semi-metal states. Our work provides a general framework for further studying topological properties of the  $D + 1$  dimensional space-time crystal.

The fundamental concept of crystal and the associated band theory based on the Bloch theorem lay the foundation of condensed matter physics. Studies on the crystal symmetry and band structure topology lead to the discoveries of topological insulators, topological superconductors, the Dirac and Weyl semi-metal states [1–3]. Periodically driving further provides a new route to engineer topological states even in systems originally topologically trivial in the absence of driving, as explored in the irradiated graphene [4, 5], semiconducting quantum wells [6], dynamically modulated cold atom optical lattices [7], and photonic systems [8, 9]. The periodicity of the quasi-energy enriches the topological band structures [10–12], such as the dynamically generated Majorana modes [13], 1D helical channels [14] and anomalous edge states associated with zero Chern number [15, 16]. Topological classifications for interacting Floquet systems have also been investigated [17–21].

For periodically driven crystals, most studies treat the temporal periodicity separately from the spatial one. In fact, the driven system can exhibit much richer symmetry structures than a simple direct product of spatial and temporal symmetries. In particular, a temporal translation at a *fractional* period can be combined with the space group symmetries to form novel space-time intertwined symmetries, which, to the best of our knowledge, have not yet been fully explored. For static crystals, the intrinsic connections between the space-group symmetries and physical properties, especially the topological phases, have been extensively studied [22–29]. Therefore, it is expected that the intertwined space-time symmetries could also protect non-trivial properties of the driven system, regardless of microscopic details.

In this article, we propose the concept of “space-time” crystal exhibiting the intertwined space-time symmetries, whose periodicities are characterized by a set of  $D + 1$  independent basis vectors, generally space-time mixed. The situation of separate spatial and temporal periodicities is a special case and is also included. The full dis-

crete space-time symmetries of space-time crystals form a class of new group structures – dubbed the “space-time” group, which is the generalization of space group by including “time-screw” and “time-glide” operations. A complete classification of the 13 space-time groups in 1+1 D is performed, and their constraints on band structure winding numbers are studied. In 2+1 D, 275 space-time groups are classified. The non-symmorphic space-time symmetry operations, similar to their static space-group counterparts, lead to the protected spectral degeneracies for driven systems, even when the instantaneous spectra are gapped at any given time.

*Space-time crystal* – We consider the time-dependent Hamiltonian  $H = P^2/(2m) + V(\mathbf{r}, t)$  in the  $D + 1$  dimensional space-time.  $V(\mathbf{r}, t)$  exhibits the intertwined discrete space-time translational symmetry as

$$V(\mathbf{r}, t) = V(\mathbf{r} + \mathbf{u}^i, t + \tau^i), \quad i = 1, 2, \dots, D + 1, \quad (1)$$

where  $(\mathbf{u}^i, \tau^i) = \mathbf{a}^i$  is a set of the primitive basis vectors. In general, the space-time primitive unit cell is not a direct product between spatial and temporal domains. There may not even exist spatial translational symmetry at any given time  $t$ , nor temporal translational symmetry at any spatial location  $\mathbf{r}$ . Consequently, the frequently used time-evolution operator of one period for the Floquet problem generally does not apply. The reciprocal lattice is spanned by the momentum-energy basis vectors  $b^i = (\mathbf{G}^i, \Omega^i)$  defined through  $b^i \cdot \mathbf{a}^j = \sum_{m=1}^D G_m^i u_m^j - \Omega^i \tau^j = 2\pi \delta^{ij}$ . The  $D + 1$  dimensional momentum-energy Brillouin zone (MEBZ) may also be momentum-energy mixed.

*Generalized Floquet-Bloch theorem* We generalize the Floquet and Bloch theorems for the time-dependent Schrödinger equation  $i\hbar \partial_t \psi(\mathbf{r}, t) = H(\mathbf{r}, t) \psi(\mathbf{r}, t)$ . Due to the space-time translation symmetry, the lattice momentum-energy vector  $\kappa = (\mathbf{k}, \omega)$  remains conserved. Only the  $\kappa$  vectors inside the first MEBZ are non-equivalent, and those outside are equivalent up to integer reciprocal lattice vectors. The Floquet-Bloch states la-

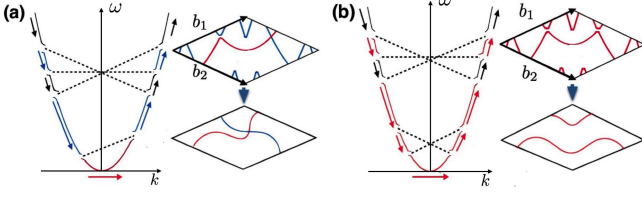


FIG. 1. Folding the band dispersions of the 1+1 D space-time crystal into the 1st rhombic MEBZ in the weak lattice limit. The momentum-energy reciprocal lattice vectors of nonzero  $V_B$ 's are represented by dashed lines. The low-energy part of the free dispersion curve evolves to closed loops. (a) Two loops with the winding numbers  $\mathbf{w}_r = (1, 0)$  (red) and  $\mathbf{w}_b = (0, 1)$  (blue). (b) An extra nonzero  $V_G$  connects two loops in (a) forming a new one with  $\mathbf{w} = \mathbf{w}_r + \mathbf{w}_b$ .

beled by  $\kappa$  take the form of

$$\psi_{\kappa,m}(\mathbf{r}, t) = e^{i(\mathbf{k} \cdot \mathbf{r} - \omega_m t)} u_m(\mathbf{r}, t), \quad (2)$$

where  $m$  marks different states sharing the common  $\kappa$ .  $u_m(\mathbf{r}, t)$  processes the same space-time periodicity as  $H(\mathbf{r}, t)$ , and is expanded as  $u_m = \sum_B c_{m,B} e^{i(\mathbf{G} \cdot \mathbf{r} - \Omega t)}$  with  $B = (\mathbf{G}, \Omega)$  taking all the momentum-energy reciprocal lattice vectors. The eigen-frequency  $\omega_m$  is determined through the eigenvalue problem defined as

$$\sum_{B'} \{[\varepsilon_0(\mathbf{k} + \mathbf{G}) - \Omega] \delta_{B,B'} + V_{B-B'}\} c_{m,B'} = \omega_m c_{m,B}, \quad (3)$$

where  $\varepsilon_0(\mathbf{k})$  is the free dispersion, and  $V_B$  is the momentum-energy Fourier component of the space-time lattice potential  $V(\mathbf{r}, t)$ . The dispersion based on Eq. 3 is represented by a  $D$ -dimensional surface in the MEBZ which is a  $D+1$  dimensional torus.

*Dispersion winding numbers* – The band structure of the space-time crystal exhibits novel features different from those of the static crystal. For simplicity, below we use the 1+1 D case for an illustration. The dispersion relation  $\omega(k)$  forms closed loops in the 2D toroidal MEBZ, each of which is characterized by a pair of winding numbers  $\mathbf{w} = (w_1, w_2)$ . Compared to the static case in which the band dispersion only winds around the momentum direction, here  $\omega(k)$  is typically not single-valued and its winding patterns are much richer. The dispersions in the limit of a weak space-time potential  $V(x, t)$  with a rhombic MEBZ are illustrated in Fig. 1 (a) and (b), with details presented in Supplemental Material (S.M.) Sect. I [30]. When folded into the MEBZ, the free dispersion curve  $\varepsilon_0(k)$  can cross at general points not just on high symmetry ones. A crossing point corresponds to two equivalent momentum-energy points related by a reciprocal vector  $\mathbf{G}$ . When  $V_G \neq 0$ , the crossing is avoided by forming a gap at the magnitude of  $2|V_G|$ . The total number of states at each  $\mathbf{k}$  is independent of the strength of  $V(x, t)$ , hence crossing can only split along the  $\omega$ -direction and  $d\omega/dk$  is always finite. Consequently,

trivial loops with the winding numbers  $(0, 0)$  are forbidden. Generally, the winding directions of the dispersion loops are momentum-energy mixed. Furthermore, different momentum-energy reciprocal lattice vectors can cross each other, leading to composite loops winding around the MEBZ along both directions as shown in Fig. 1 (b). Hence, in general all patterns  $(w_1, w_2)$  are possible except the contractible loops.

*Space-time group* – To describe the symmetry properties of the  $D+1$  dimensional space-time crystals, we propose a new group structure dubbed “space-time” group defined as the discrete subgroup of the direct product of the Euclidean group in  $D$  spatial dimensions and that along the time-direction  $E_D \otimes E_1$ . Please note that in general the space-time group cannot be factorized as the direct product between discrete spatial and temporal subgroups. It not only includes space and magnetic group transformations in the  $D$ -spatial dimensions, but also includes operations involving fractional translations along the time-direction. Since space and time are non-equivalent in the Schrödinger equation, space-time rotations are not allowed except the 2-fold case.

To be concrete, a general space-time group operation  $\Gamma$  on the space-time vector  $(\mathbf{r}, t)$  is defined as,

$$\Gamma(\mathbf{r}, t) = (R\mathbf{r} + \mathbf{u}, st + \tau), \quad (4)$$

where  $R$  is a  $D$ -dimensional point group operation,  $s = \pm 1$  and  $s = -1$  indicates time-reversal, and  $(\mathbf{u}, \tau) = \sum_i m_i a^i$  represents a space-time translation with  $m_i$  either integers or fractions. If  $\tau = 0$ ,  $\Gamma$  is reduced to a space group or magnetic group operation according to  $s = \pm 1$ , respectively. If  $\tau \neq 0$ , when  $(\mathbf{u}, \tau)$  contains fractions of  $a^i$ , new symmetry operations arise due to the dynamic nature of the crystal potential, including the “time-screw” rotation and “time-glide” reflection, which are a spatial rotation and a reflection followed by a fractional time translation, respectively. The operation of  $\Gamma$  on the Hamiltonian is defined as  $\Gamma^{-1}H(\mathbf{r}, t)\Gamma = H(\Gamma(\mathbf{r}, t))$ , or,  $\Gamma^{-1}H(\mathbf{r}, t)\Gamma = H^*(\Gamma(\mathbf{r}, t))$  for  $s = \pm 1$ , respectively. Correspondingly, the transformation  $M_\Gamma$  on the Bloch-Floquet wavefunctions  $\psi_\kappa(\mathbf{r}, t)$  is  $M_\Gamma \psi_\kappa = \psi_\kappa(\Gamma^{-1}(\mathbf{r}, t))$ , or,  $\psi_\kappa^*(\Gamma^{-1}(\mathbf{r}, t))$  for  $s = \pm 1$ , respectively.

Now we present a complete classification of the 1+1 D space-time groups. Due to the non-equivalence between spatial and temporal directions, there are no square and hexagonal space-time crystal systems. The point-group like operations are isomorphic to  $D_2$ , including reflection  $m_x$ , time reversal  $m_t$ , and their combination  $m_x m_t$ , i.e., the 2-fold space-time rotation. Consequently, only two space-time crystal systems are allowed – oblique and orthorhombic. There exist two types of glide reflections: the time-glide reflection  $g_x$ , and  $g_t$  denoted as “glide-time-reversal” is time-reversal followed by a fractional translation along the  $x$ -direction.

The above 1+1 D space-time symmetries give rise to 13 space-time groups in contrast to the 17 wallpaper

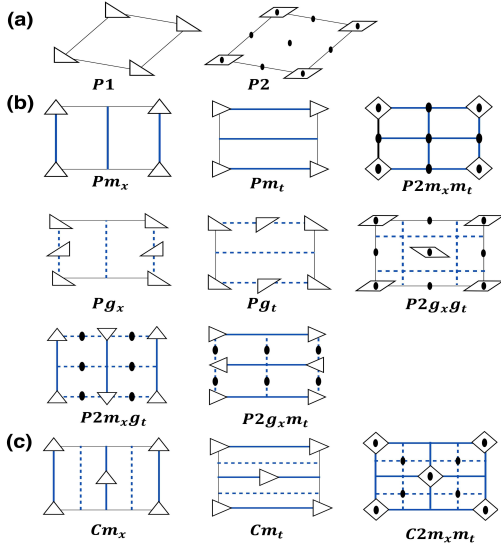


FIG. 2. The classification of 13 space-time groups in 1+1D and the associated crystal configurations. The solid oval marks the 2-fold space-time axis, and the parallelogram means the 2-fold axis without reflection symmetries. The thick solid and dashed lines represent reflection and glide-reflection axes, respectively. Configurations of triangles and the diamond denote the local symmetries under reflections. (a) The oblique lattices with and without 2-fold axes. Their basis vectors are generally space-time mixed. The primitive (b) and centered (c) orthorhombic lattices: According to their reflection and glide reflection symmetries, they are classified to 8 groups in (b), and 3 groups in (c).

space groups characterizing the 2D static crystals. The oblique Bravais lattice is simply monoclinic, while the orthorhombic ones include both the primitive and centered Bravais lattices. The monoclinic lattice gives rise to two different crystal structures with and without the 2-fold space-time axes, whose space-time groups are denoted by  $P_{1,2}$ , respectively, as shown in Fig. 2 (a). For the primitive orthorhombic lattices, the associated crystal structures can exhibit the point-group symmetries  $m_x$  and  $m_t$ , and the space-time symmetries  $g_t$  and  $g_x$ . Their combinations give rise to 8 space-time crystal structures denoted as  $Pm_x$ ,  $Pm_t$ ,  $P2m_xm_t$ ,  $Pg_x$ ,  $Pg_t$ ,  $P2g_xg_t$ ,  $P2m_xg_t$ ,  $P2g_xm_t$ , respectively, as shown in Fig. 2 (b). Four of them possess the 2-fold space-time axes as indicated by “2” in their symbols. For the centered orthorhombic Bravais lattices, 3 crystal structures exist with space-time groups denoted as  $Cm_x$ ,  $Cm_y$ , and  $C2m_xm_t$ , respectively, as shown in Fig. 2 (c). They all exhibit glide-reflection symmetries, and the last one possesses the 2-fold space-time axes as well. Two unit cells are plotted for the centered lattices to show the full symmetries explicitly, and their primitive basis vectors are actually space-time mixed.

The classifications of the space-time groups in higher dimensions are generally complicated. A general method

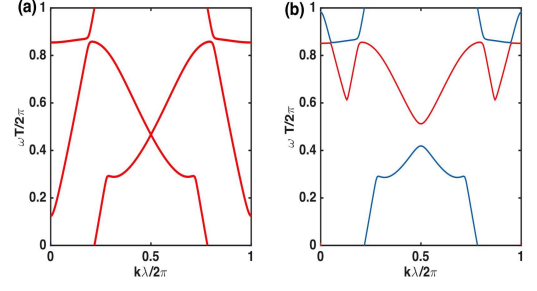


FIG. 3. (a) The Floquet-Bloch band spectrum with the space-time lattice potential possessing the glide time-reversal symmetry  $g_t$ . When applied to the states with  $\kappa_x = \pi/\lambda$ ,  $g_t$  becomes a Kramers symmetry protecting the double-degeneracy. (b) Lifting the Kramers degeneracy by adding a glide time-reversal symmetry breaking term.

is the group cohomology as presented in Sect II of S. M. [30]. In particular, the classification of 2+1D space-time group is outlined in Sect III of S. M. [30], whose structures are further enriched by spatial rotations and time-screw rotations. Compared to the 3D static crystals, the cubic crystal systems are not allowed, and two different monoclinic crystal systems appear with the perpendicular axis along the time and spatial directions, respectively. In total, there are 7 crystal systems and 14 Bravais lattices, but 275 space-time groups.

*Protection of spectral degeneracy* The intertwined space-time symmetries besides translations can protect spectral degeneracies. Below we consider the effects from the Kramers symmetry without spin and the non-symmorphic symmetries for the 1+1 D and 2+1 D space-time crystals, respectively.

Consider a 1+1 D space-time crystal whose unit cell is a direct product of spatial and temporal periods  $\lambda$  and  $T$ , respectively. We assume the system is invariant under the glide time-reversal operation  $g_t(x, t) = (x + \frac{1}{2}\lambda, -t)$ , whose operation on the Hamiltonian is defined as  $g_t^{-1}Hg_t = H^*(g_t(x, t))$ . The corresponding transformation  $M_{g_t}$  on the Bloch-Floquet wavefunction  $\psi_\kappa(x, t)$  of Eq. 2 is anti-unitary defined as  $M_{g_t}\psi_\kappa = \psi_\kappa^*(g_t^{-1}(x, t))$ . This glide time-reversal operation leaves the line of  $\kappa_x = \pi/\lambda$  in the MEBZ invariant.  $M_{g_t}$  becomes a Kramers symmetry for states with  $\kappa_x = \pi/\lambda$ ,

$$M_{g_t}^2\psi_\kappa = \psi_\kappa(x - \lambda, t) = e^{-i\kappa_x\lambda}\psi_\kappa = -\psi_\kappa, \quad (5)$$

without involving the half-integer spinor structure. It protects the double degeneracy of the momentum-energy quantum numbers of  $\psi_\kappa$  and  $M_{g_t}\psi_\kappa$ . Hence the crossing at  $\kappa_x = \pi/\lambda$  cannot be avoided and the dispersion winding numbers along the momentum direction must be even.

As a concrete example, we study a crystal potential with the above spatial and temporal periodicities,  $V(x, t) = V_0(\sin \frac{2\pi}{T}t \cos \frac{2\pi}{\lambda}x + \cos \frac{2\pi}{T}t)$ . Except the glide

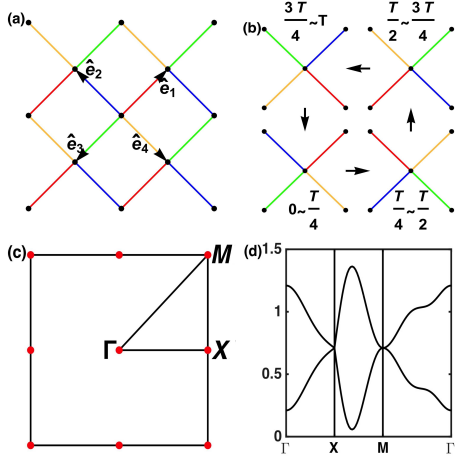


FIG. 4. (a) The 2+1 D space-time lattice structure of the Hamiltonian Eq. 7. The bond directions are marked as  $\vec{e}_{1,3} = \pm\frac{1}{2}(\hat{x} + \hat{y})$ ,  $\vec{e}_{2,4} = \mp\frac{1}{2}(\hat{x} - \hat{y})$ . (b) The time-dependent hopping pattern rotates  $90^\circ$  every one quarter period. The bonding strengths  $w_{e_i}(t)$  of the  $R$ ,  $B$ ,  $G$  and  $Y$  bonds equal 0.2, 3,  $-3.2$ , and 0.5, respectively. (c) The momentum Brillouin zone with high symmetry points  $\Gamma = (0,0)$ ,  $M = (\pm\pi, \pm\pi)$ , and  $X = (0, \pm\pi)$  and  $(\pm\pi, 0)$ . (d) The dispersions along the cuts from  $\Gamma$  to  $X$  to  $M$  to  $\Gamma$ . Two-fold degeneracies appear at  $X$  and  $M$ .

time-reversal symmetry, it does not possess other symmetries. Its Bloch-Floquet spectrum is calculated based on Eq. 3, and a representative dispersion loop is plotted in the MEBZ shown in Fig. 3 (a). The crossing at  $\kappa_x = \pi/\lambda$  is protected by the glide time-reversal symmetry giving rise to a pair of Kramers doublet. As a result, the winding number of this loop is  $\mathbf{w} = (w_x, w_t) = (2, 0)$ . If a glide time-reversal breaking term  $\delta V = V'_0 \cos(\frac{2\pi}{\lambda}x)$  is added into the crystal potential, the crossing is avoided as shown in Fig. 3 (b). Consequently, the dispersion splits into two loops, both of which exhibit the winding number  $(1, 0)$ . Similarly, out of the 8 primitive orthorhombic space-time crystals, 3 of them,  $Pg_t$ ,  $P2g_xg_t$ , and  $P2g_tm_x$ , enforce this non-spinor type Kramers degeneracy, while the other 5 generally does not protect such a degeneracy.

Next we present a 2+1 D Floquet semi-metal state, whose spectral degeneracies are protected by non-symmorphic space-time group operations. Consider that the space-time little group of the momentum  $\mathbf{k}$  contains two non-symmorphic space-time group operations  $g_{1,2}$ , both of which do not flip the time direction, hence, they are represented by unitary operators. If they satisfy

$$g_1 g_2 = T g_2 g_1, \quad (6)$$

where  $T$  is a translation of integer lattice vectors. As shown in Sect. IV in S. M. [30],  $T$  can only be a spatial translation without involving the time denoted as  $T(\mathbf{u})$ . Assume  $\mathbf{k} \cdot \mathbf{u} = 2\pi p/q$  with  $p$  and  $q$  coprime, we find that the Bloch-Floquet wavefunctions exhibit a  $q$ -fold degeneracy at the momentum-energy vector  $\kappa = (\mathbf{k}, \omega)$

proved as follows. Since  $g_1$  belongs to the little group,  $\psi_\kappa(\mathbf{r}, t)$  can be chosen to satisfy  $M_{g_1}\psi_{\kappa,1} = \mu\psi_{\kappa,1}$ , then  $\psi_\kappa, M_{g_2}\psi_\kappa, M_{g_2}^2\psi_\kappa, \dots, M_{g_2}^{q-1}\psi_\kappa$  are the common Bloch-Floquet eigenstates sharing the same  $\kappa$  but exhibiting a set of different eigenvalues of  $g_1$  as  $\eta, \mu\eta, \mu^2\eta, \dots, \mu^{q-1}\eta$  with  $\eta = e^{i\pi p/q}$ . Then they are orthogonal to each other forming a  $q$ -fold degeneracy. Compared to the case of non-symmorphic space group protected degeneracy [23, 24, 27], here  $g_{1,2}$  are space-time operations for a dynamic space-time crystal. For the case that one or both of  $g_{1,2}$  flip the time direction, the situation is more involved due to involving anti-unitary operations. Protected degeneracies are still possible as presented in Sect. IV in S. M. [30].

We employ a 2+1 D tight-binding space-time model as an example to illustrate the above protected degeneracy. A snapshot of the lattice is depicted in Fig. 4 (a), which consists of two sublattices: The  $A$ -type sites are with integer coordinates  $(i, j)$ , and each  $A$ -site emits four bonds along  $\vec{e}_i$  to its four neighboring  $B$  sites at  $(i \pm \frac{1}{2}, j \pm \frac{1}{2})$ . The space-time Hamiltonian within the period  $T$  is

$$H(t) = - \sum_{\vec{r} \in A, \vec{r} + \frac{a}{2}\vec{e}_i \in B} \{w_{\vec{e}_i}(t)c_{\vec{r}}^\dagger d_{\vec{r} + \frac{a}{2}\vec{e}_i} + h.c.\}, \quad (7)$$

where  $a$  is the distance between two nearest  $A$  sites, and  $w_{\vec{e}_i}(t)$ 's are hopping amplitudes with different strengths. Their time-dependence is illustrated in Fig. 4 (b): Within each quarter period,  $w_{\vec{e}_i}$  does not vary, and their pattern rotates  $90^\circ$  after every  $T/4$ . At each given time, the lattice possesses a simple 2D space group symmetry  $p2111$ , which only includes two-fold rotations around the  $AB$ -bond centers without reflection and glide-plane symmetries. For example, the rotation  $R_\pi$  around  $(\frac{a}{4}, \frac{a}{4})$  transforms the coordinate  $(x, y, t) \rightarrow (\frac{a}{2} - x, \frac{a}{2} - y, t)$ . In addition, there exist "time-screw" operations, say, an operation  $S$  defined as a rotation around an  $A$ -site  $(0, 0)$  at  $90^\circ$  followed by a time-translation at  $T/4$ , which transforms  $(x, y, t) \rightarrow (y, -x, t + \frac{T}{4})$ .  $R_\pi$  and  $S$  are generators of the space-time group for the Hamiltonian Eq. 7. Since  $S$  is a time-screw rotation, this space-time group is non-symmorphic. It is isomorphic to the 3D space-group  $I4_1$ , while its 2D space subgroup  $p2111$  is symmorphic. We have checked that, for a static Hamiltonian taking any of the bond configuration in Fig. 4 (b), the energy spectra are fully gapped. However, the non-symmorphic space-time group gives rise to spectral degeneracies. Its momentum Brillouin zone is depicted in Fig. 4 (c). The space-time little group of the  $M$ -point  $(\pi, \pi)$  contains both  $R$  and  $S$  satisfying  $RS = T(a\hat{y})SR = -SR$ . Similarly, the  $X$ -point  $(\pi, 0)$  is invariant under both  $R$  and  $S^2$  satisfying  $RS^2 = T(a\hat{x} + a\hat{y})S^2R = -S^2R$ . Hence, the Floquet eigen-energies are doubly degenerate at  $M$  and  $X$ -points as shown in Fig. 4 (d), showing a semi-metal structure.

In conclusion, we have studied a novel class of  $D+1$  dimensional dynamic crystal structures exhibiting the gen-



eral space-time periodicities. Their MEBZs are  $D+1$  dimensional torus and are typically momentum-energy entangled. The band dispersions exhibit non-trivial windings around the MEBZs. The space-time crystal structures are classified by space-time group, which extend space group for static crystals by incorporating time-screw rotations and time-glide reflections. In 1+1D, a complete classification of the 13 space-time groups is performed, and there exist 275 space-time groups in 2+1 D. Space-time symmetries give rise to novel Kramers degeneracy independent of the half-integer spinor structure. The non-symmorphic space-time group operations lead to protected spectral degeneracies for space-time crystals. This work sets up a symmetry framework for exploring novel properties of space-time crystals. It also serves as the starting point for future studies, for example, the dynamical topological phases of matter based on their space-time groups.

*Acknowledgments* This work is supported by AFOSR FA9550-14-1-0168. We also acknowledge the partial support from National Natural Science Foundation of China under Grants No. 11729402.

*Note added.* Upon completing this manuscript, we noticed an interesting and important work by T. Morimoto *et al.* [31] classifying Floquet topological crystalline insulators with two-fold space-time symmetries.

- 
- [1] M. Z. Hasan and C. L. Kane, *Rev. Mod. Phys.* **82**, 3045 (2010).
  - [2] X.-L. Qi and S.-C. Zhang, *Rev. Mod. Phys.* **83**, 1057 (2011).
  - [3] C. K. Chiu, J. C. Y. Teo, A. P. Schnyder, and S. Ryu, *Rev. Mod. Phys.* **88**, 1 (2016).
  - [4] T. Oka and H. Aoki, *Phys. Rev. B* **79**, 081406 (2009).
  - [5] Z. Gu, H. A. Fertig, D. P. Arovas, and A. Auerbach, *Phys. Rev. Lett.* **107**, 216601 (2011).
  - [6] N. H. Lindner, G. Refael, and V. Galitski, *Nat. Phys.* **7**, 490 (2011).
  - [7] G. Jotzu *et al.*, *Nature* **515**, 237 (2014).
  - [8] M. C. Rechtsman *et al.*, *Nature* **496**, 196 (2013).
  - [9] D. Leykam, M. C. Rechtsman, and Y. D. Chong, *Phys. Rev. Lett.* **117**, 013902 (2016).
  - [10] T. Kitagawa, E. Berg, M. Rudner, and E. Demler, *Phys. Rev. B* **82**, 235114 (2010).
  - [11] J. K. Asbóth, B. Tarasinski, and P. Delplace, *Phys. Rev. B* **90**, 125143 (2014).
  - [12] R. Roy and F. Harper, *Phys. Rev. B* **96**, 155118 (2017).
  - [13] M. Thakurathi, A. A. Patel, D. Sen, and A. Dutta, *Phys. Rev. B - Condens. Matter Mater. Phys.* **88**, 155133 (2013).
  - [14] J. C. Budich, Y. Hu, and P. Zoller, *Phys. Rev. Lett.* **118**, 105302 (2017).
  - [15] M. S. Rudner, N. H. Lindner, E. Berg, and M. Levin, *Phys. Rev. X* **3**, 031005 (2013).
  - [16] P. Titum *et al.*, *Phys. Rev. X* **6**, 021013 (2016).
  - [17] A. C. Potter and T. Morimoto, *Phys. Rev. B* **95**, 155126 (2017).
  - [18] A. C. Potter, T. Morimoto, and A. Vishwanath, *Phys. Rev. X* **6**, 041001 (2016).
  - [19] C. W. Von Keyserlingk and S. L. Sondhi, *Phys. Rev. B - Condens. Matter Mater. Phys.* **93**, 245145 (2016).
  - [20] C. W. von Keyserlingk and S. L. Sondhi, *Phys. Rev. B* **93**, 245146 (2016).
  - [21] D. V. Else and C. Nayak, *Phys. Rev. B - Condens. Matter Mater. Phys.* **93**, 201103 (2016).
  - [22] L. Fu, *Phys. Rev. Lett.* **106**, 106802 (2011).
  - [23] S. A. Parameswaran, A. M. Turner, D. P. Arovas, and A. Vishwanath, *Nat. Phys.* **9**, 299 (2013).
  - [24] S. M. Young and C. L. Kane, *Phys. Rev. Lett.* **115**, 126803 (2015).
  - [25] Z. Wang, A. Alexandradinata, R. J. Cava, and B. A. Bernevig, *Nature* **532**, 189 (2016).
  - [26] J. Kruthoff *et al.*, *Arxiv* 1612.02007 (2016).
  - [27] H. Watanabe, H. C. Po, M. P. Zaletel, and A. Vishwanath, *Phys. Rev. Lett.* **117**, 096404 (2016).
  - [28] B. Bradlyn *et al.*, *Nature* **547**, 298 (2017).
  - [29] A. Bouhon and A. M. Black-Schaffer, *Phys. Rev. B* **95**, 241101 (2017).
  - [30] See Supplemental Material for further explanations and more technical details.
  - [31] T. Morimoto, H. C. Po, and A. Vishwanath, *Phys. Rev. B* **95**, 195155 (2017).
  - [32] *International Tables for Crystallography, Volume C: Mathematical, Physical and Chemical Tables*, edited by E. Prince (International Union of Crystallography, 2004).
  - [33] H. Hiller, *Am. Math. Mon.* **93**, 765 (1986).
  - [34] *International tables for crystallography. Volume A: Space-group symmetry*, edited by M. I. Aroyo (International Union of Crystallography, 2016).